Supporting Information to "The impact of stochastic sea ice perturbations on seasonal forecasts"

Kristian Strommen[1,2,*], Michael Mayer[1,3,*], Andrea Storto[4], Jonas Spaeth[1], and Steffen Tietsche[1]

[1]European Center for Medium-range Weather Forecasts, Reading, England and Bonn, Germany.
[2]Department of Physics, University of Oxford, United Kingdom.
[3]Department of Meteorology and Geophysics, University of Vienna, Vienna, Austria
[4]Institute of Marine Sciences (ISMAR), National Research Council of Italy (CNR), Italy.
[*]These authors contributed equally to this work.

Correspondence: Kristian Strommen (kristian.strommen@ecmwf.int)

Contents

Supporting Text S1 and Supporting Figures S1 to S11.

Supporting Text S1

An idealized model of ice-atmosphere interactions is given by the following set of stochastic ordinary differential equations:

$$\frac{d}{dt}\text{ATM} = a \cdot \text{ATM} + b \cdot \text{ICE} + \xi_{\text{ATM}}, \quad (1)$$

$$\frac{d}{dt}\text{ICE} = c \cdot \text{ATM} + d \cdot \text{ICE} + \xi_{\text{ICE}}. \quad (2)$$

Here ICE can be thought of as the area-averaged SIC over a "generic" region of the Arctic, while ATM can be thought of as the component of the atmosphere which dominates the atmospheric forcing on the ice in this region. The coefficients a and d are capturing the presence of autocorrelation, while the coefficients b and c capture the presence of coupling; the ξ terms in both equations represent the residual forcing on both quantities, and are assumed to be random Gaussian processes with no temporal autocorrelation and a mean of 0. Given actual data, the coefficients can be fitted using Linear Inverse Modelling, and this model is therefore often informally referred to as a LIM model. For further details and references, see Strommen et al. (2022).

This LIM model of the atmosphere can be used to assess the interaction between stochastic ice perturbations and negative atmospheric feedbacks in coupled versus uncoupled systems. First note that a negative (positive) atmospheric feedback simply corresponds to the c coefficient being negative (positive). Then note that we can model the inclusion of stochastic ice perturbations as simply increasing the standard deviation of ξ_{ICE}, as this amounts to increasing the amount of random ice-related variability. Finally, while a coupled system can be simulated by simply initialising the LIM equations and integrating forward in time, an uncoupled system where the atmosphere is prescribed can be simulated by taking the ATM timeseries from an already generated coupled simulation, and then using this as input when integrating the ICE equations.

To test the effect of coupling in the presence of negative atmospheric feedbacks, we carry out this procedure using as our starting point the coefficients determined in Strommen et al. (2022) for the coupled Barents-Kara-NAO system. Hence $a = -2.66, b = 1.14, c = -1.52, d = -0.76$. The standard deviation of ξ_{ATM} is set to 2.4. We then set the standard deviation of ξ_{ICE} as a free parameter, and for each choice of this parameter integrate a coupled and uncoupled system for 20,000 timesteps and compute the standard deviations of the ICE timeseries generated in the two integrations. The initial 1000 steps are discarded before computing standard deviations to avoid the effect of the initial spin-up. The result is shown in Figure S8(a). It can be seen that, firstly, the temporal ice variability is consistently higher in the uncoupled system and, secondly, that the difference increases as one increases the amplitude of stochastic perturbations. This behaviour is robust to reasonable changes in the parameters, as long as $c < 0$. If $c > 0$ the opposite behaviour is seen, in that temporal variability is reduced in the uncoupled system. Similarly, we can test the effect on ensemble spread. For both the coupled and uncoupled set-ups, we first choose the value of the standard deviation of ξ_{ICE}. Then we generate 20 random initial conditions for the ICE and ATM variables by drawing from random normal distributions with mean 0 and standard deviation 2, and run 11 ensemble forecasts from each such initial condition. Then we compute the ensemble spread of the final forecasts, again discarding the initial spin-up. The result is shown in Figure S8(b). The ensemble spread is generally higher in the coupled simulations compared to the uncoupled, but ensemble spread grows faster as a function of $\sigma_{\xi_{\text{ICE}}}$ in the uncoupled simulations compared to the coupled simulations.

Thus, in this idealized system, the removal of the negative (positive) atmospheric feedback in the coupled system leads to an enhancement (reduction) of the ice variability and spread. Furthermore, this effect becomes more pronounced when the variability of the ice is greater. It follows that when one increases the overall magnitude of stochastic perturbations, for example by perturbing individual parameters with individual noise fields, this could have a big impact in uncoupled simulations but a small impact in coupled simulations.

Additional Supporting Figures

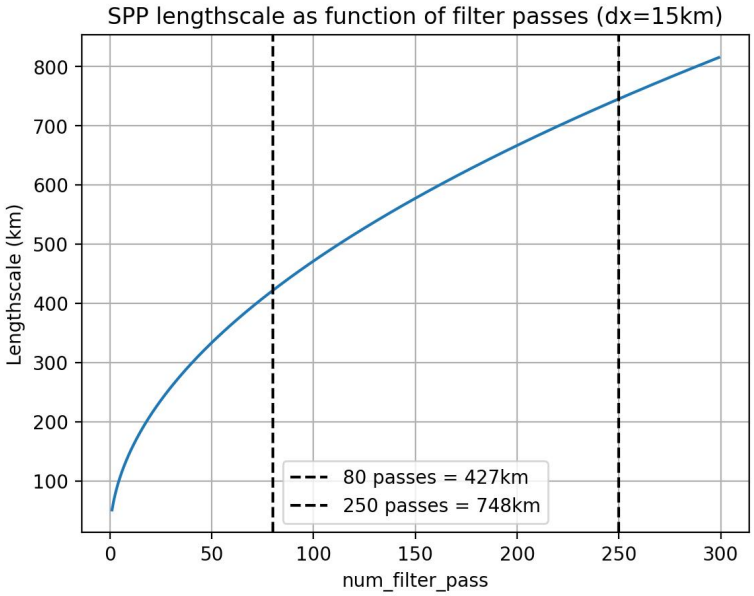

Figure S1. The SPP random noise field lengthscale (km) as a function of the number of Shapiro filter passes. For a given number of Shapiro filter passes, the estimated lengthscale is computed as $dx \cdot \pi / \arccos(exp(-1/2n))$. Here dx is the approximate gridspacing in the Arctic, which is ≈ 15km.

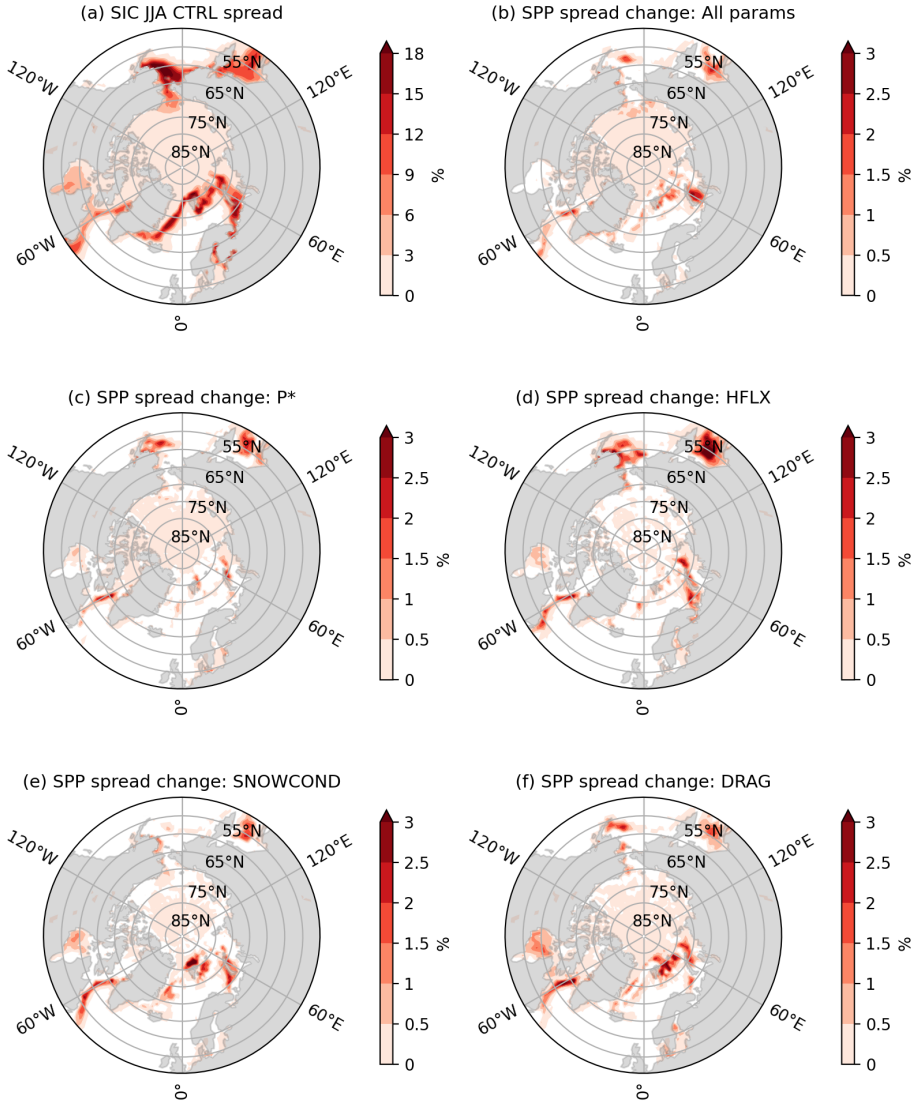

Figure S2. Impact of SPP on DJF SIC spread for single-parameter perturbations in cycle 48R2 of the IFS. In (a): DJF SIC ensemble spread in CTRL. In (b) the change in spread when perturbing all of the rn_pstar, rn_oiht, rn_cnd_s and rn_cio parameters. In (c) to (f): the change in spread when perturbing, in order, only the rn_pstar, rn_oiht, rn_cnd_s and rn_cio parameters. The ensemble forecasts cover 1993-2023 with 11 ensemble members.

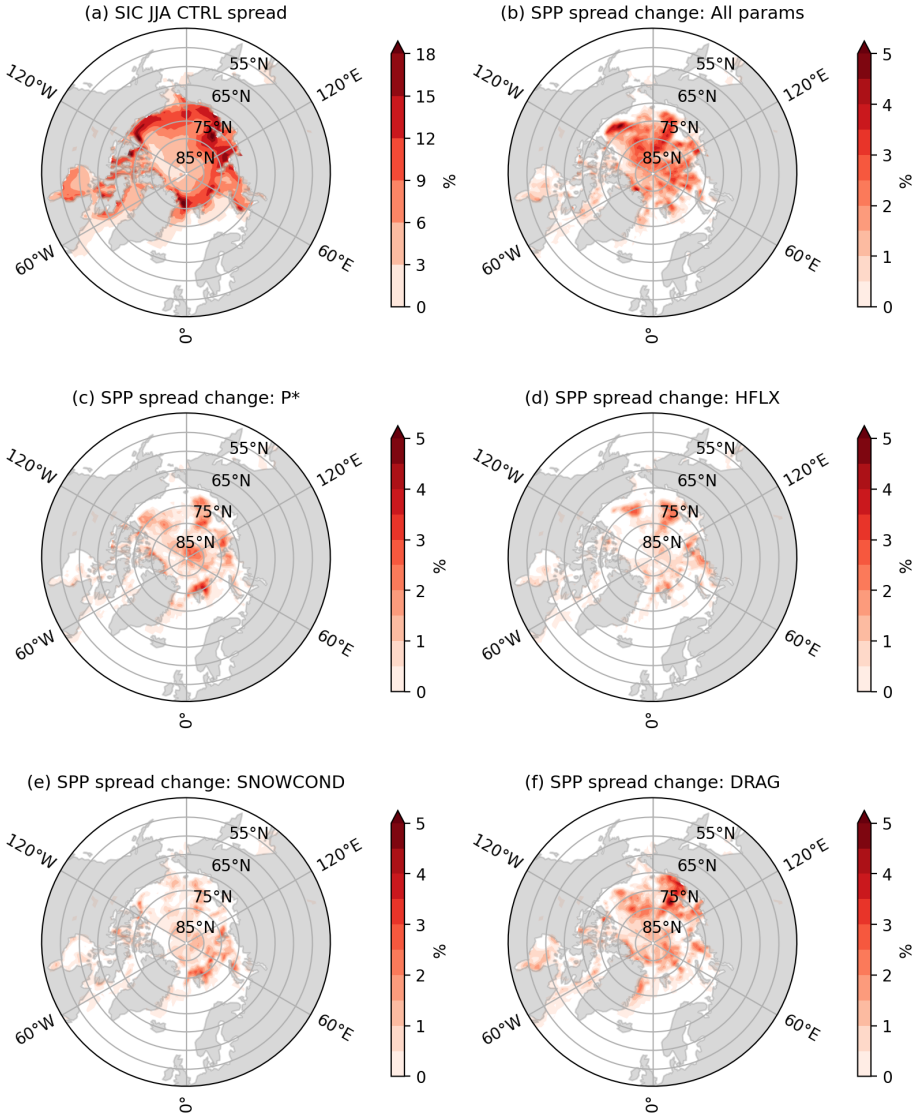

Figure S3. Impact of SPP on JJA SIC spread for single-parameter perturbations. As in Figure S2 but for JJA.

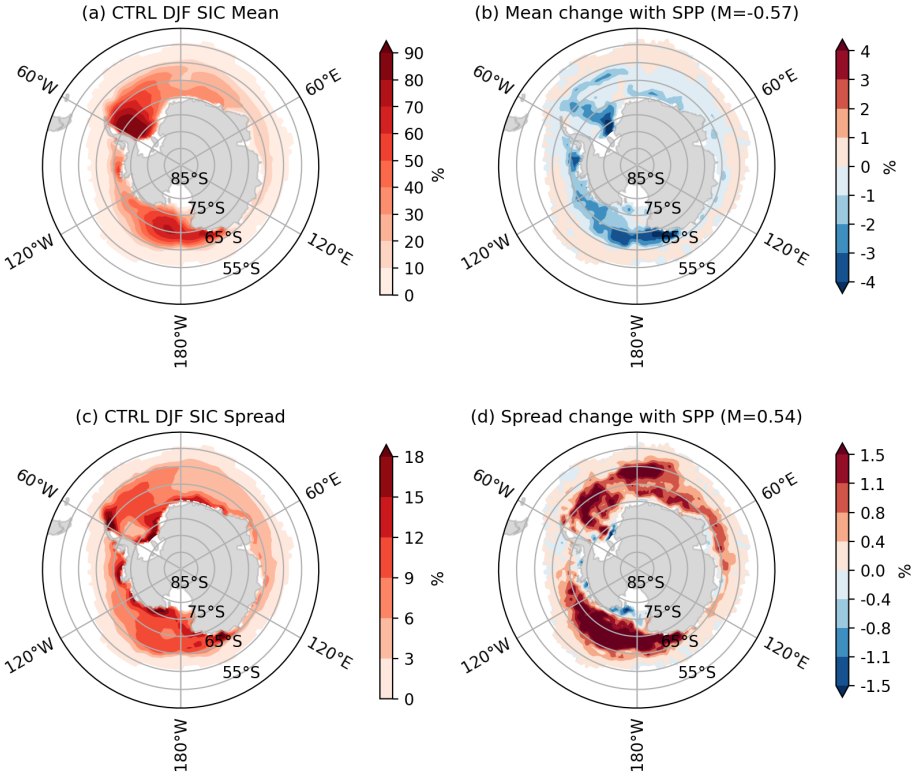

Figure S4. Impact of SPP on DJF SIC mean and spread in the Southern Hemsiphere. In (a): DJF SIC ensemble mean in CTRL. In (b): DJF SIC ensemble in SPP minus that of CTRL. In (c) and (d): the same but for DJF SIC ensemble spread.

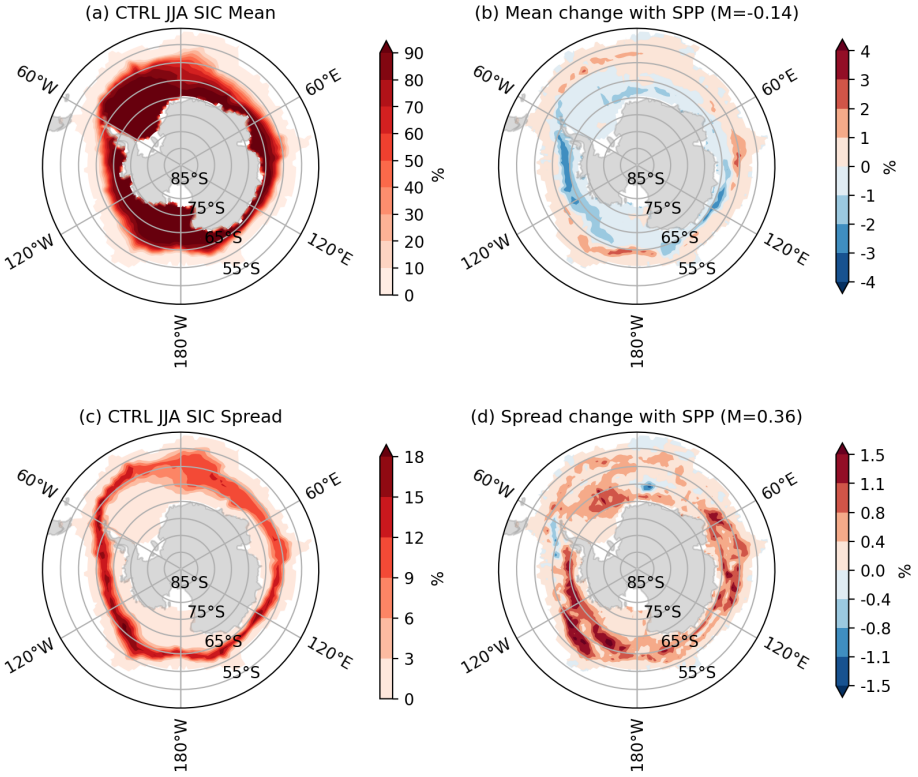

Figure S5. Impact of SPP on JJA SIC mean and spread in the Southern Hemsiphere. In (a): JJA SIC ensemble mean in CTRL. In (b): JJA SIC ensemble in SPP minus that of CTRL. In (c) and (d): the same but for JJA SIC ensemble spread.

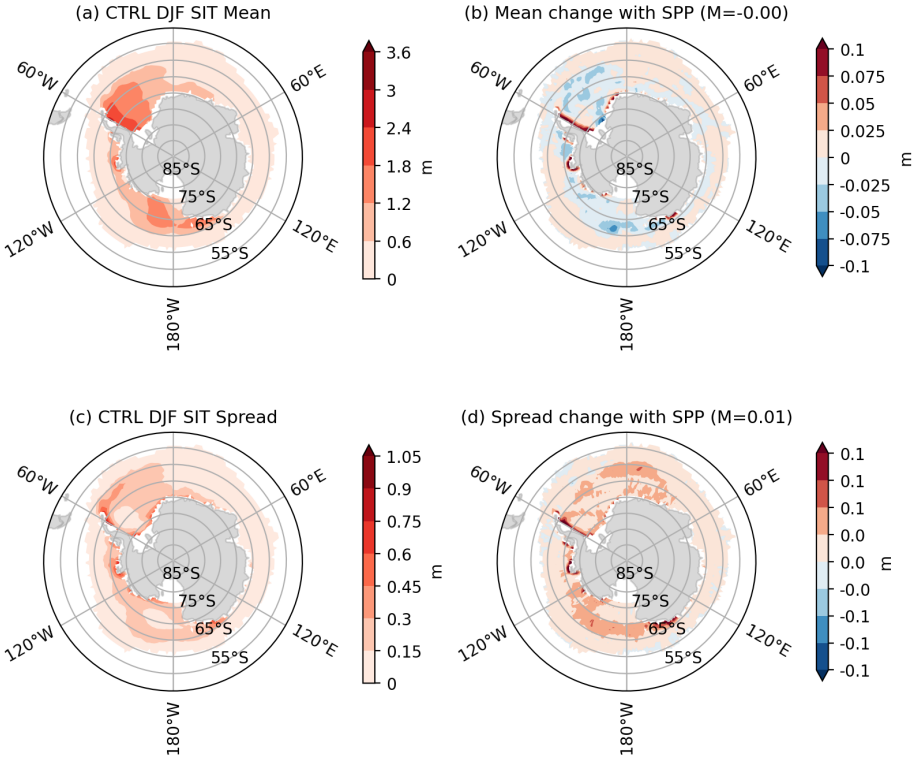

Figure S6. Impact of SPP on DJF SIT mean and spread in the Southern Hemsiphere. In (a): DJF SIT ensemble mean in CTRL. In (b): DJF SIT ensemble in SPP minus that of CTRL. In (c) and (d): the same but for DJF SIT ensemble spread.

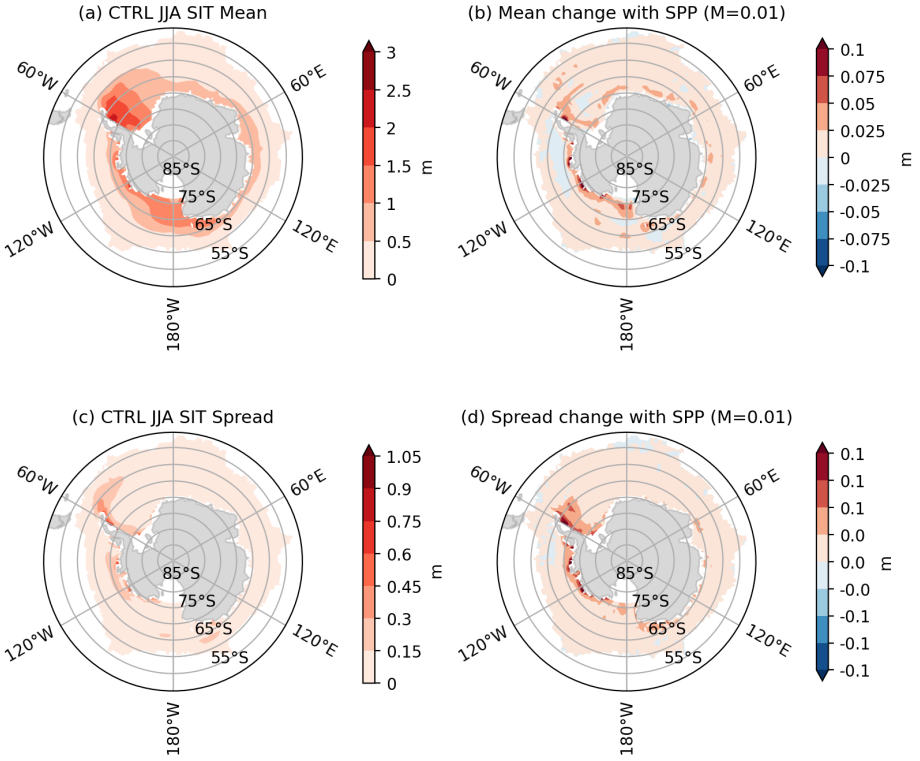

Figure S7. Impact of SPP on JJA SIT mean and spread in the Southern Hemsiphere. In (a): JJA SIT ensemble mean in CTRL. In (b): JJA SIT ensemble in SPP minus that of CTRL. In (c) and (d): the same but for JJA SIT ensemble spread.

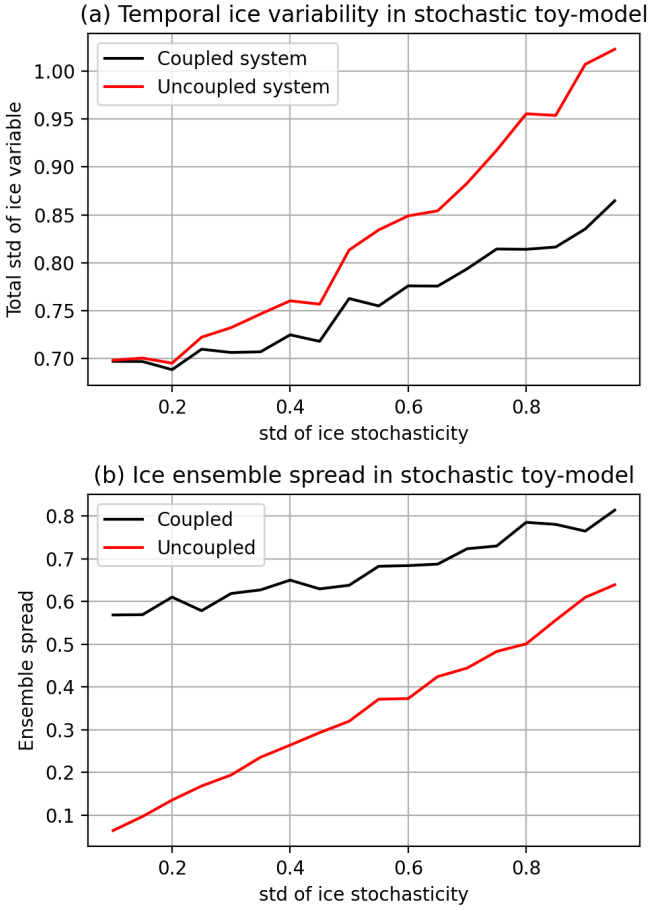

Figure S8. In (a): standard deviation of the sea ice variable as a function of the magnitude of the random ice forcing in an idealized LIM model of the ice-atmosphere system, for a coupled system (black) and uncoupled system (red). In (b): the ensemble spread in this LIM model as a function of the standard deviation of the sea ice variable. See Text S1 for details.

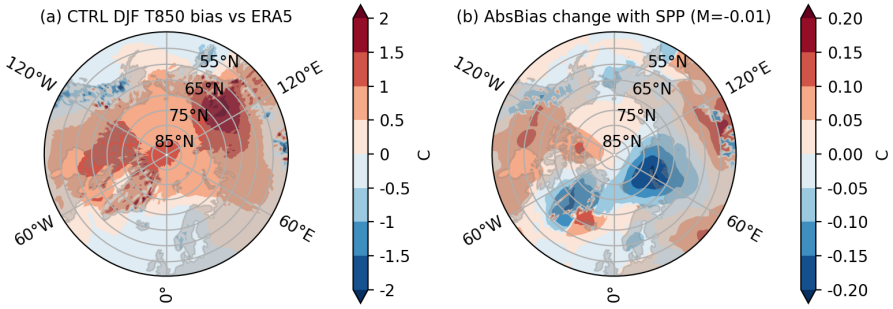

Figure S9. Impact of SPP on the T850 bias. In (a): the DJF T850 bias of CTRL, measured against ERA5. In (b): the absolute bias change with SPP. The value of M is the mean across all gridpoints in the domain.

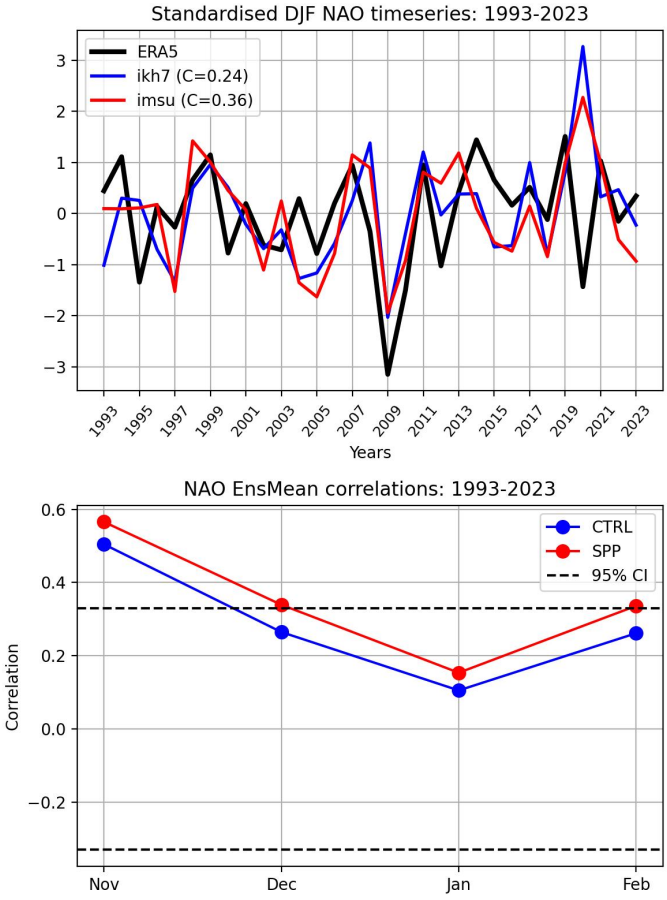

Figure S10. Impact of SPP on DJF NAO skill. Top panel: DJF NAO timeseries for ERA5, the CTRL ensemble mean (ikh7, blue line) and SPP ensemble mean (imsu, red line). The timeseries have been standardised to have mean zero and standard deviation 1. The values of C in the legend are the anomaly correlation coefficients between the ensemble means and ERA5. Bottom panel: the anomaly correlation coefficient of the ensemble means against ERA5 for each of the months in NDJF. A 95% confidence interval for the null hypothesis of no skill is given as stipled black lines; it is estimated by modelling the DJF NAO for ERA5 and CTRL as an autoregressive process with a lag of 1 year and assuming the processes are independent. The NAO is computed by computing the leading empirical orthogonal function of DJF Z500 in ERA5 over the Euro-Atlantic domain 30N-90N, 80W-40E, and then projecting the DJF Z500 in this domain for all datasets onto this pattern.

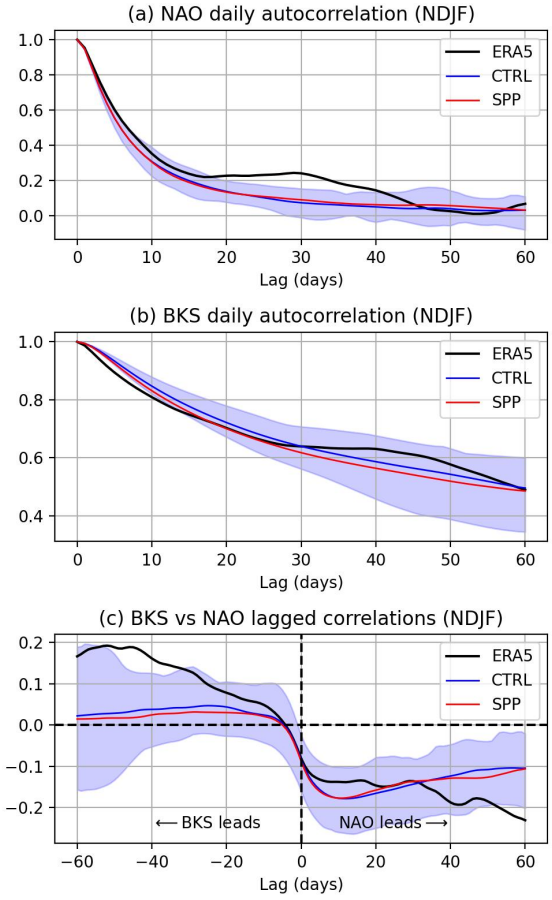

Figure S11. Coupling between Barents-Kara SIC and the NAO. In (a): the autocorrelation of the daily NAO timeseries for ERA5 (black), CTRL (blue) and SPP (red), computed over the NDJF seasons of 1993-2023, and using all ensemble members for CTRL and SPP. The blue shading shows the range spanned by individual CTRL ensemble members. In (b): the same but for BKS, i.e., the area-averaged SIC over the Barents-Kara region (67N-80N, 10E-75E). In (c): lagged correlations between the NAO and BKS.

References

Strommen, K., Juricke, S., and Cooper, F.: Improved teleconnection between Arctic sea ice and the North Atlantic Oscillation through stochastic process representation, Weather and Climate Dynamics, 3, 951–975, https://doi.org/https://doi.org/10.5194/wcd-3-951-2022, 2022.